

1 **Running Header:** Genetic architecture of water-use efficiency

2

3 **The genetic architecture of local adaptation II: The QTL landscape of water-use efficiency**
4 **for foxtail pine (*Pinus balfouriana* Grev. & Balf.)**

5

6 Andrew J. Eckert^{1*}, Douglas E. Harwood², Brandon M. Lind², Erin M. Hobson¹, Annette Delfino
7 Mix³, Patricia E. Maloney⁴, and Christopher J. Friedline¹

8

9 ¹Department of Biology, Virginia Commonwealth University, Richmond, VA 23284

10 ²Integrative Life Sciences Program, Virginia Commonwealth University, Richmond, VA 23284

11 ³Institute of Forest Genetics, USDA Pacific Southwest Research Station, Placerville, CA 95667

12 ⁴Department of Plant Pathology, University of California, Davis, CA 95616

13

14 ***Author for correspondence:**

15 Andrew J. Eckert

16 Department of Biology

17 Virginia Commonwealth University

18 Richmond, VA 23284

19 e-mail: aeckert2@vcu.edu

20 phone: +1-804-828-0800

21 fax: +1-804-828-0503

22

23

24

25

26

27
28
29
30
31
32
33
34
35
36
37
38
39
40
41
42
43
44
45
46
47
48
49
50
51

Abstract

Water availability is an important driver of the geographic distribution of many plant species, although its importance relative to other climatic variables varies across climate regimes and species. A common indirect measure of water-use efficiency (WUE) is the ratio of carbon isotopes ($\delta^{13}\text{C}$) fixed during photosynthesis, especially when analyzed in conjunction with a measure of leaf-level resource utilization ($\delta^{15}\text{N}$). Here, we test two hypotheses about the genetic architecture of WUE for foxtail pine (*Pinus balfouriana* Grev. & Balf.) using a novel mixture of double digest restriction site associated DNA sequencing, species distribution modeling, and quantitative genetics. First, we test the hypothesis that water availability is an important determinant of the geographical range of foxtail pine. Second, we test the hypothesis that variation in $\delta^{13}\text{C}$ and $\delta^{15}\text{N}$ is genetically based, differentiated between regional populations, and has genetic architectures that include loci of large effect. We show that precipitation-related variables structured the geographical range of foxtail pine, climate-based niches differed between regional populations, and $\delta^{13}\text{C}$ and $\delta^{15}\text{N}$ were heritable with moderate signals of differentiation between regional populations. A set of large-effect QTLs ($n = 11$ for $\delta^{13}\text{C}$; $n = 10$ for $\delta^{15}\text{N}$) underlying $\delta^{13}\text{C}$ and $\delta^{15}\text{N}$ variation, with little to no evidence of pleiotropy, was discovered using multiple-marker, half-sibling regression models. Our results represent a first approximation to the genetic architecture of these phenotypic traits, including documentation of several patterns consistent with $\delta^{13}\text{C}$ being a fitness-related trait affected by natural selection.

Key words: Adaptation; double digest restriction site associated DNA sequencing; ddRADSeq; foxtail pine; genetic architecture; *Pinus balfouriana*; quantitative trait locus

52 **Introduction**

53 Descriptions of the genetic components underlying fitness-related phenotypic variation
54 have been a focus of quantitative genetics for over a century (Shull 1908; Fisher 1918; Mather
55 1941; Ford 1975; Mackay *et al.* 1994; Ritland *et al.* 2011 and references therein). These
56 descriptions have progressed from identifications of the genetic elements affecting trait variation
57 (e.g. Jermstad *et al.* 2001) to analysis of interactions among these elements with one another
58 and the environment (e.g. Jermstad *et al.* 2003). Uniting all these descriptions are foundational
59 questions about the structure, function, and evolution of genotype-phenotype maps in natural
60 populations. For forest trees, these descriptions historically addressed traits of economic
61 importance such as specific gravity of wood (e.g. Groover *et al.* 1994), microfibril angle (e.g.
62 Sewell *et al.* 2000), growth (e.g. Wu 1998), and phenology (e.g. Pelgas *et al.* 2011), with the
63 ultimate goals of marker-assisted breeding (Neale and Savolainen 2004) and trait prediction
64 from genotypic data (Grattapaglia and Resende 2011). These traits, while economically
65 important, often also affect fitness (especially phenology, see Sorensen 1983), so that these
66 efforts can also be leveraged to understand the genetic basis of ecologically relevant trait
67 variation. The linkage between traits measured in common gardens and fitness in natural
68 populations, however, is usually assumed *post hoc*, which can lead to storytelling (Barrett and
69 Hoekstra 2011) and oversimplification of the ecological ramifications of quantitative genetic
70 results. Here, we address this disconnect through simultaneous use of species distribution
71 modeling and quantitative trait locus (QTL) mapping to dissect the genetic architecture of an
72 ecologically important phenotypic trait for foxtail pine (*Pinus balfouriana* Grev. & Balf).

73 The spatial and temporal distribution of all viable individuals across the Earth's
74 landscape for a given species is defined as its geographical range (Brown *et al.* 1996).
75 Evolution of range sizes and structural attributes of these ranges have been studied for a variety
76 of taxa for many decades (e.g. Mayr 1963; Antonovics 1976; Brown *et al.* 1996; Gaston 2003;
77 Eckert *et al.* 2008; Sheth and Angert 2014). The common thread underlying these interests is

Genetic architecture of water-use efficiency

78 the assumption that fitness of individuals within species is related to the known geographical
79 range for each species based on the environments defined by this range, other selective
80 pressures (i.e. competition) across this range, and the phylogeographic history that resulted in
81 the current geographical range (Hutchinson 1957; Pulliam 2000; Chuine 2010). For example,
82 relative fitness values within plant populations tend to be highest in their home environments
83 and lower in novel environments at the margin or outside of known geographical ranges
84 (reviewed in Leimu and Fischer 2008). Regardless of the relationship between this pattern and
85 evolutionary concepts such as local adaptation, it is clear that current geographical ranges are
86 to some degree projections of ecological niches (i.e. realized versus fundamental niches), or at
87 least some aspect of these niches, onto geographical space (Pulliam 2000; Ettinger *et al.* 2011).
88 Knowledge of the environmental and climatic drivers of geographical ranges can therefore be
89 informative about links between traits responsive to these drivers and fitness.

90 Species distribution models (SDMs) are commonly utilized as predictive tools with which
91 to assess the importance of environmental variables to current geographical ranges of species
92 (Elith *et al.* 2006). At a minimum, these models are built from known occurrences of a certain
93 species and the environmental and ecological attributes of these locations derived from either
94 field measurements or information stored in geographical information systems (GIS) layers.
95 Numerous approaches are available with which to build models from these data (Segurado and
96 Araujo 2004; Elith *et al.* 2006; Phillips *et al.* 2006). Once constructed, SDMs are often used
97 subsequently to study the evolutionary development of ranges (e.g. McCormack *et al.* 2010), as
98 well as the effects of continued climate change on current geographical ranges (e.g. Pearson
99 and Dawson 2003). However, there are limitations to equating SDMs, even those with good
100 predictive abilities of current geographical ranges, with realized ecological niches and hence
101 measures of fitness limits (Hampe 2004; Soberon and Peterson 2005; Warren and Seifert
102 2011). For example, individuals used to create SDMs are considered exchangeable, so that
103 fitness variation among individuals is ignored (Hampe 2004). Some of these issues, especially

Genetic architecture of water-use efficiency

104 those related to exchangeability of individuals within species, can be addressed through a
105 careful matching of modeling units (e.g. genetically differentiated populations within species;
106 *sensu* Davis *et al.* 2005), geographical scale (e.g. the geographical scale relevant to the
107 genetically differentiated populations), and the research questions of interest.

108 Water is crucial to the survival of many plant species (e.g. Sorenson 1983), although its
109 importance relative to other environmental factors varies depending upon the environmental
110 factors that are most limiting within local environments (Dudley 1996). The intrinsic efficiency by
111 which plants use water (WUE) is defined as the ratio of net assimilation of carbon from CO₂
112 during photosynthesis to the loss of water during transpiration (Bacon 2004). Carbon isotopic
113 composition ($\delta^{13}\text{C}$) is an indirect measure of intrinsic WUE and is based upon the ratio of two
114 isotopes of carbon (¹³C and ¹²C) within plant tissue standardized to a reference. This ratio is
115 related to WUE because it has been demonstrated that the discrimination by C₃ plants of ¹³CO₂
116 relative to ¹²CO₂ is correlated to the ratio of carbon assimilation during photosynthesis to
117 stomatal conductance (Farquhar *et al.* 1982; Farquhar and Richards 1984; e.g. Zhang and
118 Marshall 1994). The physiological and environmental mechanisms, however, driving the linkage
119 between $\delta^{13}\text{C}$ and intrinsic WUE at various levels of biological organization are numerous, so
120 that the expected linear relationship between $\delta^{13}\text{C}$ and WUE may not always hold (Seibt *et al.*
121 2008). For example, differences in $\delta^{13}\text{C}$ across individual plants at the leaf level can result from
122 changes in carbon to nitrogen allocation during carboxylation, variation in leaf structure and
123 morphology, and/or variation in available CO₂ (Seibt *et al.* 2008). Within a common
124 environment, however, it is assumed that variation in available amounts of atmospheric CO₂ is
125 negligible. Variation for $\delta^{13}\text{C}$ across individual plants in these common environments should
126 therefore reflect variation for intrinsic WUE. Indeed, previous research in conifers has
127 established that variation in $\delta^{13}\text{C}$ across individual plants is heritable (Seiler and Johnson 1988;
128 Cregg 1993; Brendel *et al.* 2002; Baltunis *et al.* 2008; Cumbie *et al.* 2011), is polygenic, yet

Genetic architecture of water-use efficiency

129 comprised of a mixture of large and small effect loci (Brendel *et al.* 2002; Gonzalez-Martinez *et*
130 *al.* 2008; Cumbie *et al.* 2011; Marguerit *et al.* 2014), and that it often reflects variation for
131 intrinsic WUE through leaf level assimilation (Zhang and Marshall 1994; Brendel *et al.* 2002;
132 Cumbie *et al.* 2011; Marguerit *et al.* 2014).

133 Water availability is often an important driver of tree distributions (Stephenson 1990 and
134 references therein), especially in Mediterranean climates (e.g. Baldocchi and Xu 2007; Lutz *et*
135 *al.* 2010). This importance is evident through increased tree mortality as a function of both direct
136 and indirect consequences associated with changing water availability (van Mantgem *et al.*
137 2009; Allen *et al.* 2010). Regional and local water availability will likely be altered, either through
138 changes to annual precipitation totals or the seasonality of precipitation, under most climate
139 change scenarios, especially in ecosystems dependent on residual summer snow-packs
140 (Barnett *et al.* 2005). The ability of natural populations of forest trees to respond to changing
141 water availability is linked to segregating genetic variation for traits responsive to water
142 availability (Aitken *et al.* 2008). Knowledge of the genetic architecture of such traits, therefore,
143 provides an important resource for assessing forest health, as well as the genetics of adaptation
144 (Neale and Kremer 2011). Here, we test two hypotheses about the genetic architecture of WUE
145 for foxtail pine – (i) water availability is an important determinant of the geographical range of
146 foxtail pine and hence fitness and (ii) variation in $\delta^{13}\text{C}$ and $\delta^{15}\text{N}$ is genetically based,
147 differentiated between regional populations, and has genetic architectures that include loci of
148 large effect. We subsequently discuss how the integration of results from disparate fields of
149 research (i.e. genomics, ecology, and quantitative genetics) provides information useful to
150 foundational tests about the genetic architecture of local adaptation and its evolution (*cf.*
151 Friedline *et al.* 2015).

152

153

154

155 **Materials and Methods**

156 **Focal Species**

157 Foxtail pine is one of three species classified within subsection *Balfourianae* of section
158 *Parrya* within subgenus *Strobus*. It is generally regarded as the sister taxon to Great Basin
159 bristlecone pine (*P. longaeva* D. K. Bailey; see Eckert and Hall 2006). The distribution of this
160 species is relegated to the high elevation mountains of California, with all known occurrences
161 being in either the Klamath Mountains of northern California or in the high elevations of the
162 southern Sierra Nevada (Figure S1). These two regions are separated by approximately 500 km
163 and differ in climate, soils, and forest composition (Ornduff 1974; Eckert and Sawyer 2002;
164 Barbour *et al.* 2007).

165 **Common Garden**

166 A common garden representing 141 maternal foxtail pine trees was established at the
167 Institute of Forest Genetics (Placerville, CA) during 2011 and 2012 using a randomized block
168 design. Cones were collected from 141 maternal trees sampled range-wide, with 72 sampled
169 from the Klamath Mountains and 69 from the southern Sierra Nevada region. For each maternal
170 tree, 35 – 100 seeds were germinated and grown in standard conditions as outlined in Eckert *et*
171 *al.* (2015). More information about the common garden can be obtained from Friedline *et al.*
172 (2015). Of these 141 maternal trees, offspring, assumed to be half-siblings, from five were
173 selected for analysis of water-use efficiency (see **Phenotype determination**, Table 1). The
174 megagametophyte associated with each germinated seed from these five maternal trees was
175 rescued and used to construct a high-density linkage map based on four of the five maternal
176 trees (Friedline *et al.* 2015). The seedlings from each maternal tree were allowed to grow for a
177 full year after which needles were sampled ($n = 32$ to 40/maternal tree) for determination of
178 phenotypes and genotypes. As done by Friedline *et al.* (2015), families were named using
179 colors (i.e. these were the colors of family identifier tags in the common garden), with families

Genetic architecture of water-use efficiency

180 sampled from the Klamath Mountains being labeled as blue, yellow, and purple and families
181 sampled from the southern Sierra Nevada being labeled as red and green.

182 **Phenotype Determination**

183 Two phenotypic traits were measured from needle tissue sampled from each growing
184 seedling – carbon isotope discrimination ($\delta^{13}\text{C}$) and foliar nitrogen content ($\delta^{15}\text{N}$). These were
185 chosen because ($\delta^{13}\text{C}$) is a proxy for intrinsic WUE (Farquhar *et al.* 1982; Farquhar and
186 Richards 1984), while $\delta^{15}\text{N}$ is a proxy for plant growth and resource utilization during
187 photosynthesis (Prasolova *et al.* 2000). Tissue was sampled in year 1 of growth, which was also
188 prior to formation of randomized blocks in the common garden. Given the age of the seedlings,
189 sampling of enough needle tissue for determination of phenotypes and genotypes was
190 destructive. Thus, only a subset of the seedlings per maternal tree was used. For these
191 seedlings, all available needles were sampled, cleaned and separated into those used for
192 genotype determination and those used for phenotype determination. For phenotype
193 determination, needles were placed into a mortar with liquid nitrogen and coarsely ground by
194 hand using a pestle. The resulting needle tissue was then transferred into 20 ml glass vials and
195 oven-dried at 60°C for 96 hrs. Approximately, 2 to 3 mg of ground and dried needle tissue from
196 each seedling was subsequently placed into individual wells comprising a 96 well microtiter
197 plate. Samples were analyzed for $\delta^{13}\text{C}$ and $\delta^{15}\text{N}$ at the Stable Isotope Facility at UC Davis
198 (<http://stableisotopefacility.ucdavis.edu/>). Data are presented as carbon isotope ratios for $\delta^{13}\text{C}$
199 (‰) and weight for $\delta^{15}\text{N}$ (μg).

200 **Sequence Analysis and Genotype Determination**

201 Total genomic DNA was extracted from the remaining needles from each sampled
202 seedling using Qiagen DNeasy 96 Plant Kits following the manufacturer's protocol. The resulting
203 total genomic DNA for each seedling was quantified using spectrophotometry as implemented
204 with a Thermo Scientific NanoDrop 8000. Following quantification, samples were prepared for

Genetic architecture of water-use efficiency

205 double digest restriction site associated DNA sequencing (ddRADseq) following the protocols of
206 Parchman *et al.* (2012) as implemented for foxtail pine by Friedline *et al.* (2015). All samples
207 had concentrations of total genomic DNA in the range of 15 to 60 ng/ul. In brief, this protocol
208 proceeds via restriction digests of total genomic DNA for each sample using EcoR1 and Mse1,
209 ligation of adapters that include the Illumina primer, universal M13 primers, and 8 – 10 bp
210 barcodes, PCR amplification, and size selection of the PCR amplified and ligated restriction
211 digests. In our protocol, multiplexing (i.e. pooling) occurred post PCR and size selection was
212 carried out using 1.0% agarose gels run for 1 hour at 110 volts in 1X TAE buffer. All data are
213 based on sequencing fragments in the size range of 300 to 500 bp on the Illumina HiSeq 2500.
214 DNA sequencing was performed at the VCU Nucleic Acid Research Facility
215 (<http://www.narf.vcu.edu/index.html>).

216 Raw FASTQ sequences were quality-checked and filtered as in Friedline *et al.* (2015).
217 Briefly, reads must pass a three-stage filtering procedure to be retained for downstream
218 analysis. First, if the average quality for all bases in the read was below 30, the read was
219 discarded. Second, a five-base pair sliding window was evaluated along each raw sequence.
220 Consecutive windows were retained if their mean quality was greater-than or equal-to 30. If the
221 mean score of a window fell below this threshold, the read was trimmed at this point. If the
222 length after trimming was at least 50% of the original read length, the read was kept, otherwise
223 it was discarded. Finally, if 20% of the bases in the original read had quality scores below 30,
224 the entire read was discarded, even if its average quality met the inclusion threshold. The reads
225 that passed quality filtering were demultiplexed and assigned to individual trees in one of five
226 families: Blue, Green, Purple, Red, or Yellow.

227 Sequences were aligned to the linkage map assembly (Friedline *et al.* 2015) and read
228 groups were added using Bowtie2 version 2.2.4 (Langmead and Salzberg 2012) using the `-`
229 `very-sensitive-local` set of options. Each alignment was checked and marked for PCR
230 artifacts using Picard (<http://picard.sourceforge.net>, svn 03a1d72). Variants were called using

Genetic architecture of water-use efficiency

231 the multiallelic caller from samtools version 1.1 (Li *et al.* 2009), specifying diploidy for all
232 individuals. The resulting VCF file was processed using VCFtools version 0.1.12.b (Danecek *et*
233 *al.* 2011), retaining only biallelic SNPs that mapped to positions on the linkage map defined in
234 Friedline *et. al* (2015) with quality (`--minQ`) of at least 20. All read processing and variant
235 calling pipeline code, Python 3.4.3 and R version 3.2.0 (R Core Team 2015), can be found as
236 IPython (Pérez and Granger 2007) notebooks and associated files at
237 http://www.github.com/cfriedline/foxtail_wue.

238 Once genotypes were called for all loci on the linkage map of Friedline *et al.* (2015), we
239 selected one SNP per position on the linkage map based on minimizing the amount of missing
240 data and being polymorphic in the most families. Missing genotype data were subsequently
241 imputed for each linkage group using the default settings of the program fastPHASE ver. 1.2
242 (Scheet and Stephens 2006), with families used as populations. To account for uncertainty in
243 genotype imputation, we estimated posterior probabilities of each possible genotype (i.e. 0, 1, or
244 2) at each locus using 1,000 haplotype reconstructions provided by fastPHASE, which were
245 used subsequently used as weights in a weighted average of the minor allele count. These
246 weighted averages were then rounded to the closest value (0, 1, or 2) following normal rounding
247 rules (i.e. round downward if the tenths position is less than five, otherwise round up).

248 **Species Distribution Modeling**

249 We used species distribution models (SDMs) to justify water-use efficiency as a fitness-
250 related trait and to quantify niches of each regional population relative to one another. The
251 former provides an *a priori* justification for the measured traits as ecologically relevant, while the
252 latter provides an estimate of niche differentiation between regional populations comparable to
253 the effect of region on trait differentiation (see **Quantitative Genetic Analysis**).

254 Species distribution models were used to assess the relative importance of precipitation-
255 related and temperature-related variables to the distribution of foxtail pine. We utilized the
256 approach of maximum entropy (MaxEnt; Phillips *et al.* 2006) to construct SDMs. Known

Genetic architecture of water-use efficiency

257 locations of foxtail pine within each regional population ($n = 93$ Klamath Mountains, $n = 207$
258 southern Sierra Nevada) were gathered from digitized herbarium records available through the
259 Jepson Herbarium located at the University of California, Berkeley (<http://ucjeps.berkeley.edu/>).
260 When the latitude and longitude of locations associated with these herbarium records were
261 missing, visual inspections of maps from Google Earth were used to find the best approximation
262 to the locality described on the herbarium sample. Climate data for each regional population
263 were obtained from WorldClim (<http://www.worldclim.org/>) and are represented as 19 bioclimatic
264 variables, which are functions of temperature and precipitation variables (Table S1), given at a
265 resolution of 30 arc-seconds (~1 km). The generic grid files available from the WorldClim
266 website were trimmed for each climate variable using the *raster* library in R and the following
267 geographical extent: minimum longitude: -124.0°, maximum longitude: -117.5°, minimum
268 latitude: 35.0°, maximum latitude: 42.5°. Using these trimmed grid files and the location
269 information pruned of duplicate observations ($n_{\text{pruned}} = 65$ Klamath Mountains, $n_{\text{pruned}} = 144$
270 southern Sierra Nevada), the MaxEnt software version 3.3.3k
271 (<https://www.cs.princeton.edu/~schapire/maxent/>) was used to build a SDM for each regional
272 population. MaxEnt was run using the cross-validation option for model assessment, 10
273 replicates, a maximum number of background points of 10,000, and jackknife analysis to
274 evaluate variable importance. Measures of variable importance (i.e. variable contribution and
275 permutation importance scores) and the results of the jackknife analyses were used to assess
276 the relative roles of temperature-related and precipitation-related variables to each SDM.

277 We used also used SDMs to quantify niche differentiation between regional populations
278 of foxtail pine (Warren *et al.* 2008). We tested two null hypotheses. First, we tested the null
279 hypothesis that the two SDMs were based on a single, underlying SDM common to each
280 regional population. Second, we tested the null hypothesis that the two SDMs are no more
281 differentiated than those randomly drawn from a common SDM with non-overlapping
282 geographical distributions for each regional population. Both tests are based on the D and I

283 statistics given by Warren *et al.* (2008). The former null hypothesis was tested using the
284 *niche.equivalency.test* function in the *phyloclim* library in R, while the latter null hypothesis was
285 tested using the *bg.similarity.test* function in the same R library. Both tests were based on $n =$
286 100 permutations to derive null distributions of test statistics.

287 **Quantitative Genetic Analysis**

288 We performed two sets of analyses to dissect the genetic basis of water-use efficiency
289 for foxtail pine. First, we demonstrated that variation for the measured traits was genetically
290 based using standard methods to decompose trait variance into effects of families, regions, and
291 environment (Lynch and Walsh 1998). Second, we fit single and multiple QTL models to dissect
292 the genetic basis of each trait into their genetic components using the regression methods of
293 Knott *et al.* (1996).

294 The genetic basis for each measured trait was assessed using linear models. We fit
295 three different linear models to the observed data for each trait: (1) a fixed effect model
296 containing only a grand mean (i.e. intercept), (2) a linear mixed model with a grand mean as a
297 fixed effect plus a random effect of family, and (3) a linear mixed model of a grand mean as a
298 fixed effect plus a random effect of region plus a random effect of family nested within region.
299 Uncertainty in parameter estimates from each model was assessed using parametric
300 bootstrapping ($n = 1,000$ replicated simulations) as carried out with the *simulate* function in R.
301 Models were compared using the Akaike Information Criterion (AIC), with Akaike weights used
302 to assess the conditional probabilities for each model (Burnham and Anderson 2002). If models
303 containing random effects for families or models containing random effects for regions and
304 families nested within regions fit the data better than a model with only a grand mean, then we
305 concluded that there were non-zero heritabilities for these traits. If we assume that all offspring
306 within each family were half-siblings, we could estimate narrow-sense heritability as $h^2 =$
307 $4\sigma_{\text{fam}}^2/(\sigma_{\text{fam}}^2 + \sigma_{\text{res}}^2)$, where σ_{fam}^2 is the variance due to family nested within region and σ_{res}^2 is the
308 residual variance. Given the small number of families, however, we avoided this estimation, as

Genetic architecture of water-use efficiency

309 we were interested only in detecting non-zero heritability and not precise estimation of its
310 magnitude. Linear models with fixed effects were fit using the *lm* function, while linear mixed
311 models were fit using maximum likelihood as employed in the *lmer* function of the *lme4* library of
312 R. Log-likelihood and AIC values were extracted for each fitted model using the *logLik* and *AIC*
313 functions in R, respectively.

314 The genetic basis of each trait was dissected using the least squares regression
315 approach of Knott *et al.* (1996) for outbred, half-sibling families, where probabilities of allelic
316 inheritance due to the common parent were used as predictors for each trait. Significance of the
317 regression model was determined using a *F*-test calculated at 1-cM intervals, with the
318 distribution of this statistic under a null model of no QTLs generated via a permutation scheme
319 (Churchill and Doerge 1994). The common parent in our analyses was the maternal tree, we
320 assumed that all offspring per maternal tree were half-siblings, and we used 1,000 permutations
321 to generate null distributions of *F*-statistics. Permutations were used to create null distributions
322 for *F*-statistics at the level of the entire genome (i.e. all linkage groups) and for each
323 chromosome (i.e. linkage group) separately. We initially fit models of one QTL per linkage group
324 using three significance thresholds: (1) $\alpha = 0.05$ at the level of the entire genome (major QTL),
325 (2) $\alpha = 0.01$ at the level of a particular chromosome (minor QTL), and (3) $\alpha = 0.05$ at the level of
326 a particular chromosome (suggestive QTL). For each QTL, we estimated the percent variance
327 explained (PVE) as $PVE = 4[1 - (MSE_{full}/MSE_{reduced})]$, where MSE_{full} and $MSE_{reduced}$ are the
328 mean square errors of the full and reduced models, respectively (*cf.* Everett and Seeb 2014).
329 Following Knott *et al.* (1996), estimates of PVE were scaled by $(1 - 2r)^2$, where r is the
330 recombination frequency between the marker and QTL (i.e. $r = 0.01$ for a 1-cM scan of each
331 linkage group). Uncertainty in the position of the QTL was assessed using bootstrapping ($n =$
332 1,000 replicates). For each linkage group with a statistically significant QTL, we subsequently fit
333 a model of two QTLs using the same approach, with the only differences being the use of
334 asymptotic null distributions to test the statistical significance of the observed *F*-statistics and

335 the lack of adjustments to estimates of the PVE for multiple QTL models. All analyses were
336 conducted with the HSportlets module on GridQTL ver. 3.3.0 (Seaton *et al.* 2006; Allen *et al.*
337 2012) using the linkage map for foxtail pine reported by Friedline *et al.* (2015).

338 **Results**

339 **Sequence Analysis and Genotype Determination**

340 From two lanes of HiSeq sequencing, we obtained 148,685,598 and 160,770,417 reads
341 from lane 1 (length = 101 bp, %GC = 40) and lane 2 (length = 101 bp, %GC = 41), respectively.
342 Following read filtering, we retained 77,568,370 (length = 49 - 101 bp, %GC = 40) reads from
343 lane 1 and 107,372,313 (length = 49 - 101, %GC = 40) reads from lane 2. A summary of the
344 sequencing output and quality can be found in Table 2. The highest quality and most reads
345 came from the Blue and Red families, while the Green family produced the smallest number of
346 reads. Similarly, the Blue and Red families had the highest percentages of reads mapping to the
347 assembly. The quality of reads across all families was sufficiently high, with average quality of
348 any base of approximately 38. Graphical summaries of missing data and quality metrics are
349 available in Figures S2 and S3. We filtered SNPs at the same position on the linkage map down
350 to a set of 843 loci with the least amount of missing data and polymorphism in the most families.
351 At these 843 SNPs, missing data averaged 58.0% (0% - 95.6%). Missing data were
352 subsequently imputed using the marker ordering from Friedline *et al.* (2015) and fastPHASE.

353 **Species Distribution Modeling**

354 Species distribution models were good predictors of the current geographical ranges for
355 each regional population of foxtail pine (Figures 1, S1). Estimates of the area under the receiver
356 operating characteristic curves (ROC curves) were near 1.0 for each model for both the training
357 and test set of samples (Figure S4). Exceptions to this pattern included low to moderate
358 probabilities of occurrence outside the current geographical distribution for the Klamath
359 Mountains, which were centered on the northern Sierra Nevada, and a slightly expanded range
360 north and south of the known range limits in the southern Sierra Nevada. Foxtail pine is known

Genetic architecture of water-use efficiency

361 to be absent from these regions. In both cases, the probabilities of occurrence were less, often
362 much less, than 0.40. The SDM based on the Klamath Mountains predicted a near zero
363 probability for cells within the range of the southern Sierra Nevada and vice versa.

364 Foxtail pine inhabits the cooler portions of each region in which it is currently located
365 (Figures S5 – S6). For precipitation-related variables, however, foxtail pine in the Klamath
366 Mountains inhabits slightly wetter localities relative to background localities, while in the
367 southern Sierra Nevada foxtail pine inhabits drier localities relative to background localities. The
368 climates inhabited by foxtail pine in each region also differ. In general, differences between the
369 climates inhabited by each regional population were consistent with the Klamath Mountains
370 being warmer, yet less variable in temperature throughout the year, and wetter, yet slightly more
371 variable in precipitation throughout the year, relative to the southern Sierra Nevada. For
372 example, mean annual precipitation was almost twice as high in the Klamath Mountains as in
373 the southern Sierra Nevada (1179.66 mm versus 650.03 mm, respectively), yet the distribution
374 of precipitation was slightly more variable throughout the year (e.g. precipitation of the driest
375 month: 11.78 mm versus 12.41 mm, respectively; coefficient of variation across months: 65.86
376 versus 65.02, respectively).

377 Bioclimatic variables used to predict occurrences of foxtail pine within each regional
378 population were highly correlated with one another (Figure S7). Sets of correlated variables are
379 difficult to evaluate as contributing to SDMs (Warren and Seifert 2011). We, therefore, used
380 several different measures of variable importance. Inspection of variable contribution scores
381 revealed that temperature-related and precipitation-related variables were differentially
382 important across SDMs for each region (Figure 1; Table S2). Temperature-related variables,
383 specifically mean diurnal range (Bio2), isothermality (Bio3), and maximum temperature of the
384 warmest month (Bio5), were most important for the southern Sierra Nevada population,
385 whereas precipitation-related variables, specifically precipitation of the driest quarter (Bio17)
386 and precipitation of the wettest quarter (Bio16), were most important for the Klamath Mountains

Genetic architecture of water-use efficiency

387 population. This pattern, however, was reversed when using permutation importance scores,
388 despite a moderate correlation between rankings of importance based on variable contribution
389 and permutation importance scores (Figures 2, S8; Table S4). Temperature-related variables
390 became more important for the Klamath Mountains, specifically annual temperature (Bio1),
391 while precipitation-related variables became more important for the southern Sierra Nevada
392 population, specifically precipitation seasonality (Bio15) and mean temperature of the wettest
393 quarter (Bio8). Jackknife analysis of variable importance based on AUC, test gain, and
394 regularized test gain, however, were consistent with both temperature-related and precipitation-
395 related variables as being important for the Klamath Mountains population (Figures S9 – S11).
396 For example, mean annual temperature (Bio1), maximum temperature of the warmest quarter
397 (Bio5), mean temperature of the driest quarter (Bio9), mean temperature of the warmest quarter
398 (Bio10), precipitation of the driest quarter (Bio17), and precipitation of the warmest quarter
399 (Bio18) all contributed significantly to the SDM for the Klamath Mountains population (Figure
400 S11), although no one variable contained much information that was not present in at least one
401 of the others. In contrast, jackknife analysis of variable importance based on AUC, test gain,
402 and regularized test gain were consistent with primarily temperature-related variables,
403 specifically mean annual temperature (Bio1), mean diurnal range (Bio2), maximum temperature
404 of the warmest month (Bio5), and the mean temperature of the warmest quarter (Bio10), driving
405 the SDM for the southern Sierra Nevada population (Figures S12 – S14). As with the SDM for
406 the Klamath Mountains population, however, no one variable contained information that was not
407 present in at least one of the others (Figure S14).

408 Predicted niches based on SDMs for each regional population were dissimilar, with
409 estimates of D (0.072) and I (0.258) being much closer to zero (dissimilar) than to 1 (similar)
410 (Figure S15). These differences were significant enough to reject a null model of a single shared
411 SDM common to both regional populations ($P < 0.01$ for D and I). Even if differences were
412 accounted for in the background environments of each regional population (Figure S5), the

Genetic architecture of water-use efficiency

413 predicted niches were statistically different ($P < 0.05$ for both D and I). Replicating the analyses
414 for climate variables related only to temperature or only to precipitation revealed that niche
415 divergence was stronger for precipitation-related variables ($D_{\text{precip}} = 0.074$; $I_{\text{precip}} = 0.271$) relative
416 to temperature-related variables ($D_{\text{temp}} = 0.124$, $I_{\text{temp}} = 0.376$). Therefore, regional populations of
417 foxtail pine have divergent climatic niches, with precipitation-related variables more
418 differentiated than temperature-related variables.

419 Quantitative Genetic Analysis

420 Variation across siblings measured within the common garden was genetically based for
421 each trait (Table 3). Family identifiers nested within regional populations accounted for sizeable
422 portions of the total variance for $\delta^{13}\text{C}$ ($\sigma^2_{\text{fam}}/[\sigma^2_{\text{reg}} + \sigma^2_{\text{fam}} + \sigma^2_{\text{res}}] = 24.76\%$) and $\delta^{15}\text{N}$ ($\sigma^2_{\text{fam}}/[\sigma^2_{\text{reg}} +$
423 $\sigma^2_{\text{fam}} + \sigma^2_{\text{res}}] = 24.45\%$). This was consistent with the differences among predicted family means
424 for both traits (Figure 2), which were positively correlated (Figure 3), but not significantly so
425 (Pearson's $r = 0.415$; $P = 0.487$). Regional identifiers, however, were differentially important
426 across traits, with these identifiers accounting for marginally more variance than family
427 identifiers for $\delta^{13}\text{C}$ (26.01%) but less than 10% of the total variance for $\delta^{15}\text{N}$ (Figure 2). The joint
428 effect of family and regional identifiers (i.e. the total genetic effect = $[\sigma^2_{\text{reg}} + \sigma^2_{\text{fam}}]/[\sigma^2_{\text{reg}} + \sigma^2_{\text{fam}} +$
429 $\sigma^2_{\text{res}}]$), however, was large for each trait ($\delta^{13}\text{C}$: 50.78%; $\delta^{15}\text{N}$: 29.75%). Comparisons of linear
430 models progressing from intercept only to an intercept plus families nested within regions using
431 AIC, revealed that a linear mixed model with an intercept and families was the best fit (AIC =
432 310.29 for $\delta^{13}\text{C}$; AIC = 1031.26 for $\delta^{15}\text{N}$; Table 4). Comparison to other models using AIC
433 weights, however, revealed that the most complex model of an intercept plus region plus
434 families nested within regions had a reasonably high conditional probability (AIC weight = 0.36
435 $\delta^{13}\text{C}$; AIC weight = 0.28 for $\delta^{15}\text{N}$; Table 4) relative to those for the best model ($\delta^{13}\text{C} = 0.64$; $\delta^{15}\text{N}$
436 = 0.72) for each phenotypic trait.

Genetic architecture of water-use efficiency

437 We dissected the genetic basis of the heritable variation evident for each trait from the
438 linear mixed model analysis using the regression-based approach to QTL mapping of Knott *et*
439 *al.* (1996). Application of one-locus models (i.e. a maximum of one-locus per linkage group)
440 resulted in a set of 11 QTLs across all linkage groups and both traits (Table 5; Figure 4). For
441 $\delta^{13}\text{C}$, six QTLs were discovered, with two discovered at the most stringent significance level
442 (genome-wide permutation-based $\alpha = 0.05$) and four at the least stringent significance level
443 (linkage group specific permutation-based $\alpha = 0.05$). Effect sizes for these QTLs were large to
444 moderate, with the percent variation explained (PVE) ranging from 47.807% to 24.066%. For
445 $\delta^{15}\text{N}$, five QTLs were discovered, with one QTL at the most stringent significance level, two at
446 the intermediate significance level (linkage group specific permutation-based $\alpha = 0.01$), and two
447 at the least stringent significance level. Effect sizes for these QTLs were also large to moderate,
448 with PVE varying from 39.773% to 25.058%. There was moderate autocorrelation for the *F*-
449 statistic at a resolution of 6 cM or less for $\delta^{13}\text{C}$ and 3 cM or less $\delta^{15}\text{N}$ (Figure S16), but there was
450 no correlation between *F*-statistics for each trait (Pearson's *r*: -0.014, *P* = 0.734; Figure S17). In
451 general, 95% confidence levels of positions for each QTL were large (Table 5).

452 For the 11 QTLs detected using one-locus models, 10 were consistent with multiple
453 QTLs using two-locus models (Table 6). In general, the QTLs from the one-locus models were
454 one of the pair of QTLs detected in the two-locus models. There were four exceptions to this
455 pattern, with two of these exceptions being a minor modification in position of the original QTL
456 equal to 1.0 cM. The other two exceptions included significant changes to the position of the
457 original QTL, with the QTL on linkage group 3 for $\delta^{15}\text{N}$ changing from 93.0 cM to 52.0 cM and
458 35.0 cM and the QTL on linkage group 6 for $\delta^{13}\text{C}$ changing from 0.0 cM to 46.0 cM and 56.0 cM
459 (Tables 5 and 6). The average spacing between QTLs on the same linkage group was 29.4 cM,
460 with a minimum of 3 cM to a maximum of 85 cM. The multi-QTL PVE for each trait ranged from
461 a minimum of 42.685% to a maximum of 71.315%, with only one instance of positional overlap

Genetic architecture of water-use efficiency

462 in QTLs for each trait (linkage group 3 at 34.0 cM for $\delta^{13}\text{C}$ and 35.0 cM for $\delta^{15}\text{N}$). On average,
463 there was a negative relationship between distance (cM) and the correlation of family effects
464 (Pearson's r) between QTLs on the same linkage group (Figure S18), so that strong positive
465 correlations of family effects were observed when QTLs were close together (<15 cM) and
466 strong negative correlations when QTLs were farther apart (>20 cM).

467 QTL effects from the one-locus QTL models were consistent with differentiation between
468 regional populations, with family effects opposite in sign more often than expected by chance for
469 $\delta^{13}\text{C}$ (Fisher's exact test: odds ratio = 0.113, $P = 0.009$), but not for $\delta^{15}\text{N}$ (Fisher's exact test:
470 odds ratio = 1.319, $P = 1.0$). Trait differentiation was similarly structured (Tables 3 and 4), with
471 the clearest signal of differentiation for $\delta^{13}\text{C}$. The same patterns were observed for family effects
472 in the two-locus models for the original QTL from Table 5, but not for the second QTL ($P > 0.05$
473 for both $\delta^{13}\text{C}$ and $\delta^{15}\text{N}$).

474 Discussion

475 Climate is one of the main drivers for the distribution and diversification of forest tree
476 species (MacArthur 1972; Royce and Barbour 2000; Ettinger *et al.* 2011; Alberto *et al.* 2013).
477 The relative importance of specific climate variables as drivers of natural selection, however, is
478 often assumed. For example, if a phenotypic trait is correlated to water availability in one
479 species, the same trait is often studied in a different focal species without documenting water
480 availability as having a large impact on fitness variation in the latter. The problem lies in the
481 assumption that this correlation is also indicative of similar fitness consequences across
482 species. Here, we address this issue for foxtail pine using a novel combination of species
483 distribution modeling and quantitative genetics. We illustrate the importance of water availability
484 to the distribution of foxtail pine and hence fitness, as well as describe the genetic architecture
485 of WUE, a phenotypic trait responsive to water availability, so that this trait and the markers

486 correlated to it can be used to test hypotheses about local adaptation and its genetic
487 architecture.

488 **Climate drivers of the current geographical distribution and WUE**

489 In many situations, drivers of geographical distributions for tree species are obvious. For
490 example, links between light availability, temperature, precipitation, and phenological traits are
491 commonly noted for forest trees (Howe *et al.* 2003; Chuine 2010). In other situations, however,
492 climate drivers are less clear, so that quantification of the relative importance for a suite of
493 climate variables is needed. For foxtail pine, the drivers of its current geographical distribution
494 appear to be a mixture of temperature-related and precipitation-related variables, with a clear
495 pattern that precipitation-related variables are necessary to explain the current geographical
496 range. This implies that phenotypic traits correlated to precipitation-related variables likely have
497 fitness consequences for foxtail pine, as precipitation-related variables appear to structure its
498 current range. Additionally, the importance of these drivers is differentiated between regional
499 populations, with precipitation-related variables more differentiated than temperature-related
500 variables, which mimicked differentiation of phenotypic trait values. Thus, if we leverage the
501 correlations between $\delta^{13}\text{C}$ and water availability, a crucial component of survival and hence
502 fitness, observed in other plant species (Ehleringer *et al.* 1993) and the conclusion that
503 precipitation-related variables are important for the distribution of foxtail pine, it is likely that $\delta^{13}\text{C}$
504 variation in foxtail pine is linked with fitness.

505 In general, increases in $\delta^{13}\text{C}$ reflect higher WUE (Farquhar *et al.* 1982). Inspection of
506 mean values for $\delta^{13}\text{C}$ for each region (see Figure 3), in light of the documented precipitation
507 patterns, however, appears contradictory. On average, maternal trees in the Klamath Mountains
508 had higher $\delta^{13}\text{C}$ values, which suggests higher WUE, yet precipitation is much higher in the
509 Klamath Mountains than in the southern Sierra Nevada. It is well known, however, that soil
510 properties, such as coarseness and depth to bedrock, affect available soil moisture. For

Genetic architecture of water-use efficiency

511 example, small differences in soil texture observed across the Southern Sierra Nevada Critical
512 Zone Observatory, a site not far removed from the regional population of foxtail pine in the
513 southern Sierra Nevada, result in large differences in the available soil moisture (Bales *et al.*
514 2011). Soil texture also varied by elevation, with soils at the highest elevations being coarser
515 and less developed. As such, water availability in these soils was more limited even though
516 snowfall was typically higher. Soils between regional populations of foxtail pine are
517 fundamentally different, and so is the local distribution of foxtail pine. In the Klamath Mountains,
518 soils are primarily ultramafic, while in the southern Sierra Nevada they are largely granitic.
519 Foxtail pine grows near tops of local peaks in the Klamath Mountains, whereas in the southern
520 Sierra Nevada it is distributed broadly across large swathes of high elevation sites. Thus, one
521 explanation for the apparent contradiction is that soil properties are different, so as to create
522 patterns of soil moisture not reflective of regional mean precipitation patterns. Foxtail pine in the
523 Klamath Mountains often inhabits areas with high levels of boulder cover (Eckert and Sawyer
524 2002; Eckert 2006), which are expected to house soils with less capacity to hold water over long
525 periods of time. When coupled with the higher average temperatures in the Klamath Mountains,
526 this suggests that water may be more limited throughout the year (e.g. summer drought) than
527 expected based on annual precipitation totals. Additional work, however, would be needed to
528 quantify trait variation within each regional population and correlate it to both climate and soil
529 characteristics.

530 **Genetic architecture of water-use efficiency**

531 Both $\delta^{13}\text{C}$ and $\delta^{15}\text{N}$ were consistent with non-zero heritabilities. Families and regions
532 accounted for approximately 50% of the total phenotypic variance for $\delta^{13}\text{C}$ and 30% for $\delta^{15}\text{N}$.
533 Models with effects due to families or families nested within regions were also strongly preferred
534 over models without these effects (Table 4). The effect of region, however, was highest in
535 magnitude for $\delta^{13}\text{C}$, with the variance component for region larger than that for family. This is

Genetic architecture of water-use efficiency

536 consistent with previous estimates of quantitative genetic parameters for these phenotypic traits
537 in other conifers. For example, $\delta^{13}\text{C}$ and $\delta^{15}\text{N}$ are both heritable in a variety of pine species
538 (Brendel *et al.* 2002; Baltunis *et al.* 2008; Gonzalez-Martinez *et al.* 2008; Cumbie *et al.* 2011;
539 Joao Gaspar *et al.* 2013; Marguerit *et al.* 2014; Eckert *et al.* 2015). Populations within many
540 species are also often differentiated for $\delta^{13}\text{C}$, but not for $\delta^{15}\text{N}$ (e.g. Eckert *et al.* 2015; Maloney *et*
541 *al.* unpublished). Further work, however, would be needed to precisely estimate the level of
542 differentiation for these traits, as well as to test whether this level of differentiation is larger than
543 that expected for neutral loci (i.e. this pattern is consistent with local adaptation).

544 Estimates of narrow-sense heritabilities (h^2) resulted in values greater than 1.0 for each
545 phenotypic trait no matter which model with a family effect was used (i.e. families or regions
546 plus families nested within regions). This could be due to tissue sampling occurring prior to
547 formation of randomized blocks in the common garden, as family groups would be confounded
548 with micro-environmental variation. Use of data from Eckert *et al.* (2015) and Maloney *et al.*
549 (unpublished data) for sugar pine (*P. lambertiana* Dougl.), western white pine (*P. monticola*
550 Dougl.), and whitebark pine (*P. albicaulis* Engelm.) grown at the same facility in the same
551 experimental conditions, however, reveals that block effects for $\delta^{13}\text{C}$ were present only for the
552 relatively fast growing western white pine (Type III Wald F -tests with Kenward-Rogers degrees
553 of freedom; sugar pine: $F_{1,416.49} = 3.5166$, $P = 0.06146$; western white pine: $F_{1,630.24}$, $P =$
554 0.00068 ; whitebark pine: $F_{1,452.75} = 0.0147$; $P = 0.9037$). In contrast, block had a statistically
555 significant effect on $\delta^{15}\text{N}$ for sugar pine and western white pine ($P < 0.001$), but not whitebark
556 pine ($F_{1,429.22} = 1.6252$, $P = 0.20305$). Thus, our results should be taken with caution, but family
557 effects estimated here were similar in magnitude to those from Eckert *et al.* (2015) and
558 randomized blocks tended to have no effect on the same phenotypic traits measured in
559 whitebark pine at the same facility, a species with a similar pattern of early slow growth
560 (McCune 1988).

Genetic architecture of water-use efficiency

561 If our results are indicative of true signal, effect sizes could be over-estimated on
562 average due to the small number of sampled families (Beavis 1994). To illustrate this effect, we
563 re-analyzed the data from Eckert *et al.* (2015) for sugar pine, which was grown in a common
564 garden at the same facility and measured for $\delta^{13}\text{C}$ using the same methodology, by resampling
565 smaller numbers of families ($n = 108$ families resampled in decreasing numbers from 108 to
566 three families) and estimating h^2 . As the number of sampled families decreased, estimates of
567 mean h^2 became larger (Figure S19), with a 1.5-fold increase in the mean h^2 as the number of
568 sampled families dropped from 108 to three. This is likely also the case for foxtail pine and for
569 $\delta^{15}\text{N}$. Regardless of the precise value of h^2 , it is clear that at least a moderate amount of
570 segregating genetic variation exists for this trait in natural populations of foxtail pine.

571 There was also a moderate, but statistically insignificant, positive correlation between
572 $\delta^{13}\text{C}$ and $\delta^{15}\text{N}$ (Figure 4). This has been noted in other species, such as loblolly pine (Cumbie *et*
573 *al.* 2011), although general patterns in the sign of the correlation are lacking. In this context,
574 positive correlations could indicate that WUE is determined primarily through leaf-level
575 assimilation (e.g. Johnson *et al.* 1999; Prasolova *et al.* 2005), while a negative correlation could
576 indicate that WUE is determined primarily through stomatal conductance. Despite the observed
577 positive correlation, little evidence of pleiotropy was detected, with only a single QTL on linkage
578 group 3 shared between traits. The lack of pleiotropy for these traits has been noted in several
579 other conifer species (e.g. Marguerit *et al.* 2014). Correlations between $\delta^{13}\text{C}$ and $\delta^{15}\text{N}$, or growth
580 traits more generally, can also be driven environmentally and can change depending on water
581 availability. For example, Joao Gaspar *et al.* (2013) have shown that in water limiting
582 environments $\delta^{13}\text{C}$ correlates with survival, but in less water limited environments $\delta^{13}\text{C}$
583 correlates with height growth for maritime pine (*P. pinaster* Ait.). A similar case might be
584 occurring for foxtail pine, where in the wetter Klamath Mountains $\delta^{13}\text{C}$ variation is correlated with
585 overall growth and in the more xeric southern Sierra Nevada it is correlated with survival. In this

Genetic architecture of water-use efficiency

586 context, WUE would be realized through leaf-level assimilation in the Klamath region (as in
587 Weih *et al.* 2011 for *Salix*), and through stomatal conductance in the southern Sierra Nevada.
588 Sampling more families, measurement of other traits (e.g. growth), and experimentation in
589 multiple environments, however, would be needed to test these ideas. Importantly, $\delta^{13}\text{C}$ should
590 be measured within natural populations to assess correspondence between inferences from
591 common gardens and natural populations.

592 Using one-locus QTL models, the observed segregating genetic variance for $\delta^{13}\text{C}$ was
593 dissected into two major QTLs and four suggestive QTLs (Table 5). Each QTL explained a large
594 fraction of total phenotypic variance (23.113% to 47.807%), which suggests that the genetic
595 architecture of this fitness-related trait includes loci of large effect. Under many models of
596 adaptation, however, is difficult to separate QTLs composed of a single, large-effect locus from
597 those composed of several small-effect loci (Yeaman and Whitlock 2011). The observed large
598 values of PVE may also be over-estimated (Beavis 1994), although there is precedence for
599 large effect QTLs for $\delta^{13}\text{C}$ in other species of *Pinus*, especially those distributed in water-limited
600 regions displaying moderate levels of genetic differentiation among populations. For example,
601 Marguerit *et al.* (2014) identified a QTL explaining 67% of phenotypic variance for $\delta^{13}\text{C}$ in
602 maritime pine, which is distributed across the Mediterranean regions of Europe and has
603 moderate levels of genetic structure across this range (Eveno *et al.* 2008). For foxtail pine,
604 water availability is an important driver of its current geographical distribution and genetic
605 structure is moderate to high between regional populations and among stands within regional
606 populations (Eckert *et al.* 2008, but see Oline *et al.* 2000). Furthermore, family effects for these
607 QTLs were consistent with differentiation among regions, so it is plausible that the architecture
608 discovered here for $\delta^{13}\text{C}$ largely represents genomic regions underlying trait divergence
609 between the regional populations. If this is the case, this architecture has evolved since the

Genetic architecture of water-use efficiency

610 divergence of the regional populations from their common ancestor on the order of one million
611 years ago (Eckert *et al.* 2008).

612 Summaries of the results from two-locus QTL models were largely consistent with those
613 from the one-locus models. For the 11 QTLs reported in Table 5, 10 were consistent with at
614 least two segregating QTLs. This brings the total number of QTLs to four major and seven
615 suggestive QTLs for $\delta^{13}\text{C}$ and two major, four minor, and four suggestive QTLs for $\delta^{15}\text{N}$.
616 Interestingly, the correlation of family-level effects for the two QTLs on the same linkage group
617 was negatively related to the distance between these QTLs, so that QTLs close together tended
618 to have similar patterns of family-level effects, whereas QTLs at larger distances tended to have
619 opposite family-level effects (Figure S14). This trend was uncorrelated with the difference in
620 effect sizes between QTLs. When added to the observation that family effects were often
621 consistent within regions and differentiated between regions, a likely explanation for this pattern
622 is some form of natural selection driving clustering of loci dependent on consistency of their
623 effects on a fitness-related trait. The fitness benefit of clustering, however, is related to the level
624 of gene flow (Yeaman and Whitlock 2011), so that clustering of adaptive alleles is expected
625 under high levels of gene flow, reduced recombination, and strong magnitudes of selection. This
626 is especially pronounced when genomic rearrangements are common. Inspection of the family-
627 level linkage maps from Friedline *et al.* (2015), however, revealed little evidence for clustered
628 QTLs displaying differing marker orders across families more so than random positions on the
629 linkage map. This explanation, however, is complicated given that gene flow is approximately
630 zero between these regions (Eckert *et al.* 2008) and populations of foxtail pine are unlikely to be
631 at selection – migration equilibrium due to large effective population sizes and long generation
632 times. For example, patterns of segregating ancestral variation after divergence are similar to
633 those predicted by gene flow (Pamilo and Nei 1988), so that it becomes difficult to separate
634 pattern from process with regard to the effects of gene flow on adaptive genetic architectures.

Genetic architecture of water-use efficiency

635 Additional work within natural populations, including fine mapping of trait values in the linkage
636 bins defined by Friedline *et al.* (2015), would be needed to test these ideas further.

637 We leveraged the annotations of contigs at or near (± 3 cM) the estimated QTL positions
638 to search for putatively functional genes as the drivers of the genotype-phenotype correlations
639 for each QTL (Table S3). Annotations for foxtail pine contigs were derived through similarity
640 searches against the loblolly pine genome. Annotations were obtained from any locus on a
641 loblolly pine scaffold containing a significant hit to a RADtag from foxtail pine, with significance
642 justified by the estimated substitution rate and divergence time between these species (Friedline
643 *et al.* 2015). Several statistically significant QTLs had no annotation information available. For
644 example, the QTL on linkage group 1 for $\delta^{13}\text{C}$ had no annotations available within a 6-cM
645 window encapsulating the QTL, despite 24 of 76 RADtags having significant similarity to
646 scaffolds in loblolly pine. This is consistent with reports of gene densities reported for conifers
647 (Nystedt *et al.* 2013; Neale *et al.* 2014). For the QTL related to $\delta^{13}\text{C}$ on linkage group 2 (Table
648 5), however, two of the 18 RADtags for foxtail pine had sequence similarity to loblolly pine
649 scaffolds, with annotated InterPro domains suggestive of loci encoding stress responsive
650 proteins (Table S3; Toka *et al.* 2010; Karijolic *et al.* 2015). Another example of potentially
651 biologically informative results included the QTL on linkage group 9 for $\delta^{15}\text{N}$ where putative
652 homologs for proteins with domains such as ribosomal protein L38e, cytochrome P450, and
653 thiolase were present. Proteins containing these domains have been implicated in lipid turnover
654 during leaf senescence (Troncoso-Ponce *et al.* 2013), as well as plant growth and drought
655 stress response (Tamiru *et al.* 2015). Care should be taken in interpreting these results,
656 however, as QTL intervals were wide, annotations were based on statements of homology with
657 gene predictions in an early release of the loblolly pine genome sequence (Wegrzyn *et al.*
658 2014), and *post hoc* explanations linking gene products to phenotypic traits is prone to
659 storytelling (Barrett and Hoekstra 2011; Pavlidis *et al.* 2012). It is important to note, however,

660 that these concerns are with interpretations of putative functions of genes located within the
661 QTL as sensible in their effect on the measured phenotypic trait, and not with the biological
662 signal of linkage driving the discovery of the QTL.

663 **Conclusions**

664 We have used a mixture of species distribution modeling and quantitative genetics to
665 test two hypotheses about WUE, as measured by $\delta^{13}\text{C}$, for foxtail pine. We showed that
666 precipitation-related variables structured the geographical range of foxtail pine, that climate-
667 based niches differed between regional populations, and that similar patterns were apparent for
668 $\delta^{13}\text{C}$, which was also demonstrated to be heritable. We subsequently dissected this heritability
669 into a set of large-effect QTLs ($n = 21$ total, with 11 for $\delta^{13}\text{C}$ and 10 for $\delta^{15}\text{N}$), which we interpret
670 in light of population genetic theory about local adaptation. While we cannot definitely say that
671 WUE, as measured by $\delta^{13}\text{C}$, contributes to local adaptation, we have described to a first
672 approximation its genetic architecture, while noting several patterns consistent with $\delta^{13}\text{C}$ being a
673 fitness-related trait affected by natural selection. These are useful results with which to generate
674 further hypotheses about the evolution of genetic architecture contributing to local adaptation in
675 natural populations (e.g. Holliday *et al.* 2015). Our results also shed light on ecologically
676 relevant phenotypic trait variation useful for management decisions and predictions for range
677 shifts under changing climates.

678

679

680

681

682

683

684 **Acknowledgements** – We are grateful to the staff at the USDA Institute of Forest Genetics for
685 space and logistical support in the establishment of the common garden, as well as the staff at
686 the VCU Nucleic Acids Research Facility and Center for High Performance Computing for help
687 in generating and analyzing the Illumina short read data. Seeds for foxtail pine were obtained
688 from Tom Blush and Tom Burt. Rodney Dyer, Christopher Gough, William Eggleston and
689 Salvatore Agosta all made helpful comments on D. E. Harwood’s M.S. thesis at VCU, which
690 was the basis for this work.

691

692 **Data Archiving Statement**

- 693 • **Genotype data** are available as raw short read data as part of NCBI BioProject
694 PRJNA310118, processed short read data in VCF format (File S1), and imputed data in
695 a tab-delimited text file (File S2).
- 696 • **Phenotypic trait data** are available for all half-siblings within each of the five families
697 used for QTL mapping in a tab-delimited text file (File S3).
- 698 • **Location data** used for species distribution modeling are available in a tab-delimited text
699 file (File S4).

700

701 **References**

- 702 Aitken SN, Yeaman S, Holliday JA, Wang T, Curtis-McLane S (2008) Adaptation, migration or
703 extirpation: climate change outcomes for tree populations. *Evol Appl* 1:95-111.
- 704 Alberto FJ, Aitken SN, Alia R, Gonzalez-Martinez SC, Hanninen H, et al. (2013) Potential for
705 evolutionary responses to climate change – evidence from tree populations. *Glob Chang*
706 *Biol* 19:1645-1661.
- 707 Allen CD, Macalady AK, Chenchouni H, Bachelet D, McDowell N, et al. (2010) A global
708 overview of drought and heat-induced tree mortality reveals emerging climate change
709 risks for forests. *Forest Ecol Manag* 259:660-684.

Genetic architecture of water-use efficiency

- 710 Allen J, Scott D, Illingworth M, Dobrzelecki B, Virdee D, Thorn S, Knott S (2012) CloudQTL:
711 Evolving a Bioinformatics Application to the Cloud. Digital Research 2012, September
712 10-12, 2012. Oxford, UK.
- 713 Antonovics J (1976) The nature of limits to natural selection. *Ann Mo Bot Gard* 63:224-247.
- 714 Bacon MA (2004) Water use efficiency in plant biology. In: Bacon MA (ed) *Water Use Efficiency*
715 in Plant Biology, Blackwell Publishing Ltd, Oxford, UK, pp 1-26.
- 716 Baldocchi DD, Xu L (2007) What limits evaporation from Mediterranean oak woodlands – the
717 supply of moisture in the soil, physiological control by plants or the demand by the
718 atmosphere? *Adv Water Res* 30:2113-2122.
- 719 Bales RC, Hopmans J, O'Green AT, Meadows M, Hartsough PC, Kirchner P, Hunsaker CT,
720 Beaudette D (2011) Soil moisture response to snowmelt and rainfall in a Sierra Nevada
721 mixed-conifer forest. *Vadose Zone J* 10:786-799.
- 722 Baltunis BS, Martin TA, Huber DA, Davis JM (2008) Inheritance of foliar stable carbon isotope
723 discrimination and third-year height in *Pinus taeda* clones on contrasting sites in Florida
724 and Georgia. *Tree Genet Genomes* 4:797-807.
- 725 Barbour M, Keeler-Wolf T, Schoenherr AA (2007) *Terrestrial Vegetation of California*. Third
726 edition. University of California Press, Berkeley, California, USA.
- 727 Barnett TP, Adam JC, Lettenmaier (2005) Potential impacts of a warming climate on water
728 availability in snow-dominated regions. *Nature* 438:303-309.
- 729 Barrett RD, Hoekstra HE (2011) Molecular spandrels: tests of adaptation at the genetic level.
730 *Nat Rev Genet* 12:767-780.
- 731 Beavis WD (1994) The power and deceit of QTL experiments: Lessons from comparative QTL
732 studies. In: *Proceedings of the 49th Annual Corn and Sorghum Industry Research*
733 *Conference*, 250–266. American Seed Trade Association, Washington, DC, USA.
- 734 Brendel O, Pot D, Plomion C, Rozenberg P, Guehl J-M (2002) Genetic parameters and QTL
735 analysis of $\delta^{13}\text{C}$ and ring width in maritime pine. *Plant Cell Environ* 25:945-953.

Genetic architecture of water-use efficiency

- 736 Brown JH, Stevens GC, Kaufman DM (1996) The geographic range: size, shape, boundaries,
737 and internal structure. *Annu Rev Ecol Syst* 27:597-623.
- 738 Burnham KP, Anderson DR (2002) Model Selection and Multimodal Inference – A Practical
739 Information-Theoretic Approach. Springer, New York, New York, USA.
- 740 Chuine I (2010) Why does phenology drive species distribution? *Philos Trans R Soc Lond B Biol*
741 *Sci* 365:3149-3160.
- 742 Churchill GA, Doerge RW (1994) Empirical threshold values for quantitative trait
743 mapping. *Genetics* 138:963-971.
- 744 Cregg, BM 1993. Seed source variation in water relations, gas exchange, and needle
745 morphology of mature ponderosa pine trees. *Can J For Res* 23:749-755.
- 746 Cumbie WP, Eckert A, Wegrzyn J, Whetten R, Neale D, Goldfarb B (2011) Association genetics
747 of carbon isotope discrimination, height and foliar nitrogen in a natural population of
748 *Pinus taeda* L. *Heredity* 107:105-114.
- 749 Danecek P, Auton A, Abecasis G, *et al.* (2011) The variant call format and VCFtools.
750 *Bioinformatics* 27:2156-2158.
- 751 Davis MB, Shaw RG, Etterson JR (2005) Evolutionary responses to changing climate. *Ecology*
752 86:1704-1714.
- 753 Dudley SA (1996) Differing selection on plant physiological traits in response to environmental
754 water availability: a test of adaptive hypotheses. *Evolution* 50:92-102.
- 755 Eckert AJ (2006) Influence of substrate type and microsite availability on the persistence of
756 foxtail pine (*Pinus balfouriana*, Pinaceae) in the Klamath Mountains, California. *Am J*
757 *Bot* 93:1615-1624.
- 758 Eckert AJ, Sawyer JO (2002) Foxtail pine importance and conifer diversity in the Klamath
759 Mountains and southern Sierra Nevada, California. *Madroño* 49:33-45.

Genetic architecture of water-use efficiency

- 760 Eckert AJ, Hall BD (2006) Phylogeny, historical biogeography, and patterns of diversification
761 for *Pinus* (Pinaceae) – Phylogenetic tests of fossil-based hypotheses. Mol Phylogenet
762 Evol 40:166-182.
- 763 Eckert AJ, Tearnse BR, Hall BD (2008) A phylogeographical analysis of the range disjunction for
764 foxtail pine (*Pinus balfouriana*, Pinaceae): the role of Pleistocene glaciation. Mol
765 Ecol 17:1983-1997.
- 766 Eckert AJ, Maloney PE, Vogler DR, Jensen CE, Delfino Mix A, Neale DB (2015) Local
767 adaptation at fine spatial scales: an example from sugar pine (*Pinus lambertiana*,
768 Pinaceae). Tree Genet Genomes 11:42.
- 769 Eckert CG, Samis KE, Loughheed SC (2008) Genetic variation across species' geographical
770 ranges: the central-marginal hypothesis and beyond. Mol Ecol 17:1170-1188.
- 771 Ehleringer JR, Hall AE, Farquhar GD (1993) Stable isotopes and plant carbon/water relations.
772 Academic Press, San Diego, California, USA.
- 773 Elith J, Graham CH, Anderson RP, Dudik M, Ferrier S, et al. (1996) Novel methods improve
774 prediction of species' distributions from occurrence data. Ecography 29:129-151.
- 775 Ettinger AK, Ford KR, HilleRisLambers J (2011) Climate determines upper, but not lower,
776 altitudinal range limits of Pacific Northwest conifers. Ecology 92:1323-1331.
- 777 Eveno E, Collada, Angeles Guevara M, Leger V, Soto A, et al. (2008) Contrasting patterns of
778 selection at *Pinus pinaster* Ait. drought stress candidate genes as revealed by genetic
779 differentiation analyses. Mol Biol Evol 25:417-437.
- 780 Everett MV, Seeb JE (2014) Detection and mapping of QTL for temperature tolerance and body
781 size in Chinook salmon (*Oncorhynchus tshawytscha*) using genotyping by sequencing.
782 Evol Appl 7:480-492.
- 783 Farquhar GD, Richards RA (1984) Isotopic composition of plant carbon correlates with water-
784 use efficiency of wheat genotypes. Aust J Plant Physiol 11:539-552.

Genetic architecture of water-use efficiency

- 785 Farquhar GD, O'Leary MH, Berry JA (1982) On the relationship between carbon isotope
786 discrimination and the intercellular carbon dioxide concentrations in leaves. Aust J Plant
787 Physiol 9:121-137.
- 788 Fisher RA (1918) The correlation between relative on the supposition of Mendelian inheritance.
789 Philos T R Soc Edinburgh 52:399-433.
- 790 Ford EB (1975) Ecological Genetics, 4th edition. Chapman and Hall, London, UK.
- 791 Friedline CJ, Lind BM, Hobson EM, Harwood DE, Delfino Mix A, Maloney PE, Eckert AJ (2015)
792 The genetic architecture of local adaptation I: the genomic landscape of foxtail pine
793 (*Pinus balfouriana* Grev. & Balf.) as revealed from a high-density linkage map. Tree
794 Genet Genomes 11:49.
- 795 Gaston KJ (2003) The Structure and Dynamics of Geographic Ranges. Oxford University Press,
796 Oxford, UK.
- 797 Gonzalez-Martinez SC, Huber D, Ersoz E, Davis JM, Neale DB (2008) Association genetics in
798 *Pinus taeda* L. II. Carbon isotope discrimination. Heredity 101:19-26.
- 799 Grattapaglia D, Resende MDV (2011) Genomic selection in forest tree breeding. Tree Genet
800 Genomes 7:241-255.
- 801 Groover A, Devey M, Fiddler T, Lee J, Megraw R, Mitchell-Olds T, Sherman B, Vujcic S,
802 Williams C, Neale DB (1994) Identification of quantitative trait loci influencing wood
803 specific gravity in an outbred pedigree of loblolly pine. Genetics 138:1293-1300.
- 804 Hampe A (2004) Bioclimate envelope models: what they detect and what they hide. Global Ecol
805 Biogeogr 13:469-471.
- 806 Holliday JA, Zhou L, Bawa R, Zhang M, Oubida RW (2015) Evidence for extensive parallelism
807 but divergent genomic architecture of adaptation along altitudinal and latitudinal
808 gradients in *Populus trichocarpa*. New Phyt 209: 1240-1251.

Genetic architecture of water-use efficiency

- 809 Howe GT, Aitken SN, Neale DB, Jermstad KD, Wheeler NC, Chen THH (2003) From genotype
810 to phenotype: unraveling the complexities of cold adaptation in forest trees. *Can J Bot*
811 81:1247-1266.
- 812 Hutchinson GE (1957) Concluding remarks. *Cold Spring Harb Symp Quant Biol* 22:415-427.
- 813 Jermstad KD, Bassoni DL, Wheeler NC, Anekonda TS, Aitken SN, Adams WT, Neale DB
814 (2001) Mapping of quantitative trait loci controlling adaptive traits in coastal Douglas-fir.
815 II. Spring and fall cold-hardiness. *Theor Appl Genet* 102:1152-1158.
- 816 Jermstad KD, Bassoni DL, Jech KS, Ritchie GA, Wheeler NC, Neale DB (2003) Mapping of
817 quantitative trait loci controlling adaptive traits in coastal Douglas-fir. III. Quantitative trait
818 loci-by-environment interactions. *Genetics* 165:1489-1506.
- 819 Joao Gaspar M, Velasco T, Feito I, Alia R, Majada J (2013) Genetic variation of drought
820 tolerance in *Pinus pinaster* at three hierarchical levels: a comparison of induced osmotic
821 stress and field testing. *PLoS ONE* 8:e79094.
- 822 Johnson KH, Flanagan LB, Huber DA, Major JE (1999) Genetic variation in growth, carbon
823 isotope discrimination, and foliar N concentration in *Picea mariana*: analyses from a half-
824 diallel mating design using field-grown trees. *Can J For Res* 29:1727-1735.
- 825 Karijolic J, Yi C, Yu Y-T (2015) Transcriptome-wide dynamics of RNA pseudouridylation. *Nat*
826 *Rev Mol Cell Biol* 16:581-585.
- 827 Knott SA, Elsen, JM, Haley CS (1996) Methods for multiple-marker mapping of quantitative trait
828 loci in half-sib populations. *Theor Appl Genet* 93:71–80.
- 829 Langmead B, Salzberg SL (2012) Fast gapped-read alignment with Bowtie 2. *Nat Meth* 9:357-
830 359.
- 831 Lemiu R, Fischer M (2008) A meta-analysis of local adaptation in plants. *PLoS ONE* 3:e4010.
- 832 Li H, Handsaker B, Wysoker A, *et al.* (2009) The Sequence Alignment/Map format and
833 SAMtools. *Bioinformatics* 25:2078-2079.

Genetic architecture of water-use efficiency

- 834 Lutz JA, van Wagendonk JW, Franklin JF (2010) Climatic water deficit, tree species ranges,
835 and climate change in Yosemite National Park. *J Biogeogr* 37:936-950.
- 836 Lynch M, Walsh B (1998) *Genetics and Analysis of Quantitative Traits*. Sinauer Associates, Inc.,
837 Sunderland, Massachusetts, USA.
- 838 MacArthur RH (1984) *Geographical Ecology: Patterns in the Distribution of Species*. Princeton
839 University Press, Princeton, New Jersey, USA.
- 840 Mackay TF, Fry JD, Lyman RF, Nuzhdin SV (1994) Polygenic mutation in *Drosophila*
841 *melanogaster*: estimates from response to selection of inbred strains. *Genetics* 136:937-
842 951.
- 843 Marguerit E, Bouffier L, Chancerel E, Costa P, Lagane F, Guehl J-M, Plomion C, Brendel O.
844 The genetics of water-use efficiency and its relation to growth in maritime pine. *J Exp*
845 *Bot* 65:4757-4768.
- 846 Mather K (1941) Variation and selection of polygenic characters. *J Genetics* 41:159-193.
- 847 Mayr E (1963) *Animal Species and Evolution*. Belknap Press, Cambridge, Massachusetts, USA.
- 848 McCormack JE, Zellmer AJ, Knowles LL (2010) Does niche divergence accompany allopatric
849 divergence in *Aphelocoma* jays as predicted under ecological speciation?: Insights from
850 tests with niche models. *Evolution* 64:1231-1244.
- 851 McCune B (1988) Ecological diversity in North American pines. *Am J Bot* 75:353-368
- 852
- 853 Neale DB, Savolainen O (2004) Association genetics of complex traits in conifers. *Trends Plant*
854 *Sci* 9:325-330.
- 855 Neale DB, Kremer A (2011) Forest tree genomics: growing resources and applications. *Nat Rev*
856 *Genet* 12:111-122.
- 857 Neale DB, Wegrzyn JL, Stevens KA, Zimin AV, Puiu D, et al. (2014) Decoding the massive
858 genome of loblolly pine using haploid DNA and novel assembly strategies. *Genom Biol*
859 15:R59.

Genetic architecture of water-use efficiency

- 860 Nystedt B, Street NR, Wetterbom A, Zuccolo A, Lin Y-C, et al. (2013) The Norway spruce
861 genome sequence and conifer genome evolution. *Nature* 497:579-584.
- 862 Oline DK, Mitton JB, Grant MC (2000) Population and subspecific genetic differentiation in the
863 foxtail pine (*Pinus balfouriana*). *Evolution* 54:1813-1819.
- 864 Ornduff R (1974) *Introduction to California Plant Life*. University of California Press, Berkeley,
865 California, USA.
- 866 Pamilo P, Nei M (1988) Relationships between gene trees and species trees. *Mol Biol Evol*
867 5:568-583.
- 868 Parchman TL, Gompert Z, Mudge J, Schilkey FD, Benkman CW, Buerkle CA (2012) Genome-
869 wide association genetics of an adaptive trait in lodgepole pine. *Mol Ecol* 21:2991-3005.
- 870 Pavlidis P, Jensen JD, Stephan W, Stamatakis A (2012) A critical assessment of storytelling:
871 Gene Ontology categories and the importance of validating genomic scans. *Mol Biol*
872 *Evol* 29:3237-3248.
- 873 Pearson RG, Dawson TP (2003) Predicting the impacts of climate change on the distribution of
874 species: are bioclimate envelope models useful? *Global Ecol Biogeogr* 12:361-371.
- 875 Pelgas B, Bousquet J, Merimans PG, Ritland K, Isabel N (2011) QTL mapping in white spruce:
876 gene maps and genomic regions underlying adaptive traits across pedigrees, years and
877 environments. *BMC Genomics* 12:145.
- 878 Pérez F, Granger BE (2007) IPython: A System for Interactive Scientific Computing. *Comput Sci*
879 *Eng* 9:21-29.
- 880 Phillips SJ, Anderson RP, Schapire RE (2006) Maximum entropy modeling of species
881 geographic distributions. *Ecol Model* 190:231-259.
- 882 Prasolova NV, Xu ZH, Farquhar GD, Saffigna PG, Dieters MJ (2000) Variation in canopy $\delta^{13}\text{C}$ of
883 8-year-old hoop pine families (*Araucaria cunninghamii*) in relation to canopy nitrogen
884 concentration and tree growth in subtropical Australia. *Tree Physiol* 20:1049-1055.

Genetic architecture of water-use efficiency

- 885 Prasolova NV, Lundkvist K, Xu ZH (2005) Genetic variation in foliar nutrient concentration in
886 relation to foliar carbon isotope composition and tree growth with clones of the F1 hybrid
887 between slash pine and Caribbean pine. For Ecol Manag 210:173–191.
- 888 Pulliam HR (2000) On the relationship between niche and distribution. Ecol Lett 3:349-361.
- 889 R Core Team (2015) R: A language and environment for statistical computing. R Foundation for
890 Statistical Computing, Vienna, Austria. URL: <http://www.R-project.org/>
- 891 Ritland K, Krutovsky KV, Tsumura Y, Pelgas B, Isabel N, Bousquet J (2011) Genetic mapping in
892 conifers. In: Plomion C, Bousquet J, Kole C (eds) Genetics, Genomics and Breeding of
893 Conifers, CRC Press, New York, USA, pp 196-238.
- 894 Royce EB, Barbour MG (2000) Mediterranean climate effects. II. Conifer growth phenology
895 across a Sierra Nevada ecotone. Am J Bot 88:919-932.
- 896 Scheet P, Stephens M (2006) A fast and flexible statistical model for large-scale population
897 genotype data: applications to inferring missing genotypes and haplotypic phase. Am J
898 Hum Genet 78:629-644.
- 899 Seaton G, Hernandez J, Grunchev JA, White I., Allen J, De Koning DJ, Wei W, Berry D, Haley
900 C, Knott S (2006) GridQTL: A Grid Portal for QTL Mapping of Compute Intensive
901 Datasets. Proceedings of the 8th World Congress on Genetics Applied to Livestock
902 Production, August 13-18, 2006. Belo Horizonte, Brazil.
- 903 Segurado P, Araujo MB (2004) An evaluation of methods for modelling species distributions. J
904 Biogeogr 31:1555-1568.
- 905 Seibt U, Rajabi A, Griffiths H, Berry JA (2008) Carbon isotopes and water use efficiency: sense
906 and sensibility. Oecologia 155:441-454.
- 907 Seiler JR, Johnson JD (1988) Physiological and morphological response of three half-sib
908 families of loblolly pine to water-stress conditioning. For Sci 34:487-495.
- 909 Sewell MM, Bassoni DL, Megraw RA, Wheeler NC, Neale DB (2000) Identification of QTLs
910 influencing wood property traits in loblolly pine (*Pinus taeda* L.). I. Physical wood

Genetic architecture of water-use efficiency

- 911 properties. *Theor Appl Genet* 101:1273-1281.
- 912 Sheth SN, Angert AL (2014) The evolution of environmental tolerance and range size: a
913 comparison of geographically restricted and widespread *Mimulus*. *Evolution* 68:2917-
914 2931.
- 915 Shull GH (1908) The composition of a field of maize. *Am Breeders Assoc Rep* 5:51-59.
- 916 Soberon J, Peterson AT (2005) Interpretation of models of fundamental ecological niches and
917 species' distributional areas. *Biodiversity Informatics* 2:1-10.
- 918 Sorenson FC (1983) Geographic variation in seedling Douglas-fir (*Pseudotsuga menziesii*) from
919 the western Siskiyou Mountains of Oregon. *Ecology* 64:696-702.
- 920 Stephenson NL (1990) Climatic control of vegetation distribution - the role of the water balance.
921 *Am Nat* 135:649-670.
- 922 Tamiru M, Undan JR, Takagi H, Abe A, Yoshida K, et al. (2015) A cytochrome P450, OsDSS1,
923 is involved in growth and drought stress responses in rice (*Oryza sativa* L.). *Plant Mol*
924 *Biol* 88:85-99.
- 925 Toka I, Planchais S, Cabassa C, Justin AM, De Vos D, Richard L, et al. (2010) Mutations in the
926 hyperosmotic stress-responsive mitochondrial BASIC AMINO ACID CARRIER2 enhance
927 proline accumulation in *Arabidopsis*. *Plant Physiol.* 152:1851-1862.
- 928 Troncoso-Ponce MA, Cao X, Yang Z, Ohlrogge JB (2013) Lipid turnover during senescence.
929 *Plant Sci* 205-206:13-19.
- 930 van Mantgem PJ, Stephenson NL, Byrne JC, Daniels LD, Franklin JF, et al. (2009) Widespread
931 increase of tree mortality rates in the western United States. *Science* 323:521-524.
- 932 Warren DL, Glor RE, Turelli M (2008) Environmental niche equivalency versus conservatism:
933 quantitative approaches to niche evolution. *Evolution* 62:2868-2883.
- 934 Warren DL, Seifert SN (2011) Ecological niche modeling in Maxent: the importance of model
935 complexity and the performance of model selection criteria. *Ecol Appl* 21:335-342.

Genetic architecture of water-use efficiency

- 936 Wegrzyn JL, Liechty JD, Stevens KA, Wu L-S, Loopstra CA, et al. (2014) Unique features of the
937 loblolly pine (*Pinus taeda* L.) megagenome revealed through sequence annotation.
938 Genetics 196:891-909.
- 939 Weih M, Bonosi L, Ghelardini L, Ronnberg-Wastljung AC (2011) Optimizing nitrogen economy
940 under drought: increased leaf nitrogen is an acclimation to water stress in willow (*Salix*
941 spp.). Ann Bot 108:1347-1353.
- 942 Wu RL (1998) Genetic mapping of QTLs affecting tree growth and architecture in *Populus*:
943 implication for ideotype breeding. Theor Appl Genet 96:447-457.
- 944 Yeaman S, Whitlock MC (2011) The genetic architecture of adaptation under migration-
945 selection balance. Evolution 65:1897-1911.
- 946 Zhang J, Marshall JD (1994) Population differences in water-use efficiency of well-watered and
947 water-stressed western larch seedlings. Can J Forest Res 24:92-99.

948

949 **Compliance with Ethical Standards**

- 950 • **Disclosure of potential conflicts of interest:** Funding for this work was provided from
951 Virginia Commonwealth University (start-up funds awarded to A. J. Eckert) and from the
952 National Science Foundation (NSF-NPGI-PRFB-1306622 awarded to C. J. Friedline).
- 953 • **Research involving Human Participants and/or Animals:** There were no human
954 participants or animals used in this research.
- 955 • **Informed consent:** There were no human participants used in this research, so
956 informed consent is not applicable.

957

958

959

960

961

Genetic architecture of water-use efficiency

962 **Table 1.** Summary of the families ($n = 5$) used for QTL mapping

	Red	Green	Purple	Blue	Yellow
Latitude	36.448075	36.448075	41.319871	41.195910	41.748267
Longitude	-118.170644	-118.170644	-122.479184	-122.792240	-123.133233
Elevation (m)	3352.80	3352.80	2397.56	2103.12	2103.12
Siblings ^a	35	40	34	40	32
Locality	Cottonwood	Cottonwood	Mt. Eddy	East Boulder	Lake
	Pass	Pass		Lake	Mountain
Region	SN	SN	KM	KM	KM

963 ^aThese counts represent the numbers of siblings genotyped and phenotyped for each family.

964 Additional siblings for each family are still growing within the common garden (see **Materials**
965 **and Methods**).

966

967

968

969

970

971

972

973

974

975

976

977

978

979

Genetic architecture of water-use efficiency

980 **Table 2.** Mean and standard deviation (in parentheses) of read metrics by family

Family	Number of reads	Length (bp)	Quality	% Aligned
Blue	1,092,446 (319,903)	89.0 (8.28)	38.0 (1.05)	31.00 (4.881)
Green	691,141 (119,272)	87.6 (10.32)	37.5 (1.16)	26.08 (1.614)
Purple	724,998 (126,585)	88.1 (9.98)	37.6 (1.15)	24.81 (1.398)
Red	1,289,156 (304,551)	89.0 (8.10)	38.1 (1.05)	33.14 (3.577)
Yellow	952,597 (377,357)	88.6 (9.17)	37.8 (1.12)	28.89 (4.185)

981
982
983
984
985
986
987
988
989
990
991
992
993
994
995
996
997
998

Genetic architecture of water-use efficiency

999 **Table 3.** Attributes of linear mixed models used to estimate familial and regional effects for each
1000 phenotypic trait. Values in parentheses are 95% parametric bootstrap confidence intervals (see
1001 **Materials and Methods**).

Model Attribute	$\delta^{13}\text{C}$	$\delta^{15}\text{N}$
$\log L$	-151.705 (-167.029 – -130.520)	-512.587 (-528.588 – -491.444)
Intercept	-30.755 (-31.439 – -30.075)	21.519 (18.615 – 24.596)
Family variance component (σ^2_{fam})	0.159 (0.002 – 0.432)	7.826 (0.000 – 17.521)
Region variance component (σ^2_{reg})	0.167 (0.000 – 0.538)	1.696 (0.000 – 9.933)
Residual variance component (σ^2_{res})	0.316 (0.249 – 0.384)	22.486 (17.927 – 27.912)

1002

1003

1004

1005

1006

1007

1008

1009

1010

1011

1012

Genetic architecture of water-use efficiency

1013 **Table 4.** Comparisons of linear mixed models using the Akaike Information Criterion (AIC) by
1014 trait were used to select the best model (bolded text). In these models, the intercept was a fixed
1015 effect, while families nested within regions and regions were random effects.

Model	$\delta^{13}\text{C}$		$\delta^{15}\text{N}$	
	AIC	AIC weight ^a	AIC	AIC weight ^a
Intercept	408.10	3.66×10^{-22}	1071.76	1.16×10^{-9}
Intercept + family	310.29	0.64	1031.26	0.72
Intercept + family + region	311.41	0.36	1033.17	0.28

1016 ^aThe AIC weight is calculated using the standardized relative likelihoods, where the relative
1017 likelihood is given as $e^{(-0.5 \times \Delta\text{AIC})}$. For this calculation, ΔAIC is the difference between the AIC for
1018 each model and the AIC for the best model (bolded text), where the best model is the one with
1019 the lowest AIC. The weights are then calculated as each of relative likelihoods over the sum of
1020 the relative likelihoods, thus making the sum of the weights equal to 1. Akaike weights can also
1021 be considered as the conditional probabilities for each model.

1022

1023

1024

1025

1026

1027

1028

1029

1030

1031

1032

1033

Genetic architecture of water-use efficiency

1034 **Table 5.** Summary of QTLs for each trait that survive multiple test corrected significance
 1035 thresholds at either the level of the whole genome ($\alpha = 0.05$ for $G_{0.05}$) or a chromosome ($\alpha =$
 1036 0.01 for $C_{0.01}$, $\alpha = 0.05$ for $C_{0.05}$)

Trait	LG ^a	Position (cM)	<i>F</i>	PVE ^b (PVE _c)	Threshold <i>F</i> ^c	95% CI ^d (cM)
$\delta^{15}\text{N}$	1	0.0	4.422	26.540 (25.489)	3.818 ($C_{0.05}$)	0.0 – 97.0
$\delta^{13}\text{C}$	1	98.0	7.506	49.778 (47.807)	5.803 ($G_{0.05}$)	13.0 – 99.0
$\delta^{13}\text{C}$	2	78.0	6.040	39.139 (37.589)	5.803 ($G_{0.05}$)	3.0 – 78.0
$\delta^{13}\text{C}$	3	34.0	4.356	26.092 (25.058)	3.456 ($C_{0.05}$)	13.0 – 93.0
$\delta^{15}\text{N}$	3	93.0	4.475	27.065 (25.993)	3.725 ($C_{0.05}$)	14.0 – 93.0
$\delta^{13}\text{C}$	5	64.0	4.659	28.625 (27.491)	4.008 ($C_{0.05}$)	17.0 – 103.0
$\delta^{13}\text{C}$	6	0.0	4.198	24.825 (23.842)	3.835 ($C_{0.05}$)	0.0 – 85.0
$\delta^{15}\text{N}$	7	62.0	6.351	41.413 (39.773)	6.091 ($G_{0.05}$)	16.0 – 89.0
$\delta^{15}\text{N}$	8	72.0	5.784	37.182 (35.710)	5.559 ($C_{0.01}$)	1.0 – 100.0
$\delta^{15}\text{N}$	9	95.0	5.924	38.237 (36.809)	4.958 ($C_{0.01}$)	9.0 – 95.0
$\delta^{13}\text{C}$	12	23.0	4.105	24.066 (23.113)	4.072 ($C_{0.05}$)	15.0 – 91.0

1037 ^aLG, Linkage group

Genetic architecture of water-use efficiency

1038 ^bPVE, percent variance explained; PVE_c, corrected percent variance explained

1039 ^cThe threshold value for the *F*-statistic under the null model as determined using the listed value of α
1040 (0.05 or 0.01) and permutations following Churchill and Doerge (1994) for either individual linkage groups
1041 (C) or the entire genome (G).

1042 ^d95% CI, 95% confidence interval determined through bootstrap analysis ($n = 1,000$ replicates)

1043

1044

1045

1046

1047

1048

1049

1050

1051

1052

1053

1054

1055

1056

1057

1058

1059

1060

1061

1062

1063

1064

1065

Genetic architecture of water-use efficiency

1066 **Table 6.** Summary of two QTL models fit to each significant QTL from Table 4. Bolded *P*-values
 1067 are less than 0.05.

Trait	LG ^a	Position 1 (cM)	Position 2 (cM)	<i>F</i>	<i>P</i>	PVE ^b
$\delta^{15}\text{N}$	1	0.0	79.0	3.89	0.0023	54.518
$\delta^{13}\text{C}$	1	98.0	13.0	2.92	0.0149	64.725
$\delta^{13}\text{C}$	2	77.0	66.0	3.76	0.0030	61.685
$\delta^{13}\text{C}$	3	34.0	14.0	3.18	0.0091	44.459
$\delta^{15}\text{N}$	3	52.0	35.0	4.24	0.0012	57.594
$\delta^{13}\text{C}$	5	64.0	88.0	1.81	0.1135	37.745
$\delta^{13}\text{C}$	6	46.0	56.0	3.84	0.0026	48.892
$\delta^{15}\text{N}$	7	62.0	80.0	4.69	0.0005	71.315
$\delta^{15}\text{N}$	8	71.0	68.0	2.57	0.0287	49.661
$\delta^{15}\text{N}$	9	95.0	64.0	2.90	0.0155	53.602
$\delta^{13}\text{C}$	12	23.0	43.0	3.20	0.0088	42.685

1068 ^aLG, Linkage group

1069 ^bPVE, percent variance explained by both QTLs

1070

1071

1072

1073

1074

1075

1076

Figure Legends

1077
1078
1079 **Figure 1.** Species distribution models (SDMs) created using MaxEnt are good predictors of the
1080 current geographical range of foxtail pine (inlaid maps; AUC = area under the receiver operating
1081 characteristic curve). Precipitation and temperature-related variables are differentially important,
1082 as measured by variable contributions to each model, to the SDM of each regional population of
1083 foxtail pine, with precipitation-related variables more important for the Klamath Region and
1084 temperature-related variables more important for the southern Sierra Nevada. Variable
1085 contribution scores (± 1 standard deviation derived from 10 replicated runs of MaxEnt per
1086 SDM) are uncorrelated (Spearman's $\rho = -0.065$). For symbols without apparent error bars, the
1087 diameter of the circle was greater than the standard deviation.

1088
1089 **Figure 2.** Ranks of variable importance (low rank = more important) based on variable
1090 contribution (VC) scores and permutation importance (PI) scores to the SDM for each regional
1091 population are moderately correlated ($r =$ Spearman's ρ). Variable types are denoted using filled
1092 circles, with black used for temperature-related variables, white for precipitation-related
1093 variables, and gray for variables related to both temperature and precipitation.

1094
1095 **Figure 3.** Familial and regional level means (± 1 standard error) by trait (left: $\delta^{13}\text{C}$, right: $\delta^{15}\text{N}$)
1096 are differentiated across families and regions relative to the global mean. Dashed gray lines
1097 give global means across all families for each trait. Estimates for the Klamath Mountains (KM)
1098 are given as filled circles, while estimates for the southern Sierra Nevada (SN) are given as
1099 filled triangles. Familial names are given as colors (see **Materials and Methods**).

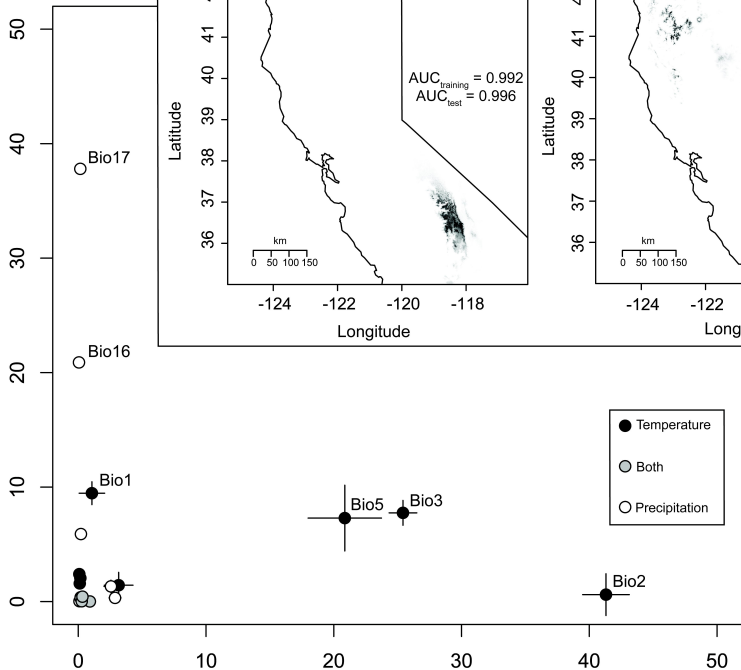
1100
1101 **Figure 4.** The relationship between traits based on family means (± 1 standard error) is
1102 positive (Pearson's $r = 0.415$), although statistically non-significant at $\alpha = 0.05$ ($P = 0.487$).
1103 Dashed gray lines give global means across all families for each trait.

Genetic architecture of water-use efficiency

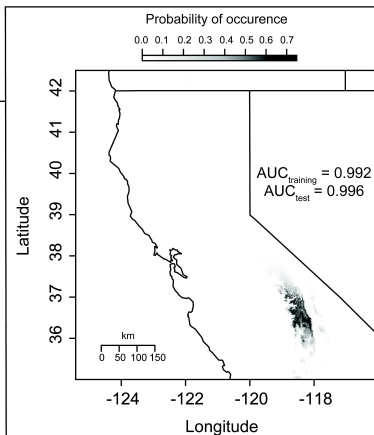
1104

1105 **Figure 5.** The distributions of the F -statistic derived from single QTL models across each
1106 linkage group for carbon isotope discrimination and nitrogen content of needles reveals the
1107 isolated nature of QTLs. The dashed horizontal line in each panel is the genome-wide
1108 significance threshold ($\alpha = 0.05$) for the F -statistic based on the permutation scheme ($n = 1,000$
1109 permutations) suggested by Churchill and Doerge (1994). Significant QTLs are denoted with
1110 filled circles ($\alpha = 0.05$, genome-wide), filled triangles ($\alpha = 0.01$, chromosome-wide) or filled
1111 squares ($\alpha = 0.05$, chromosome-wide).

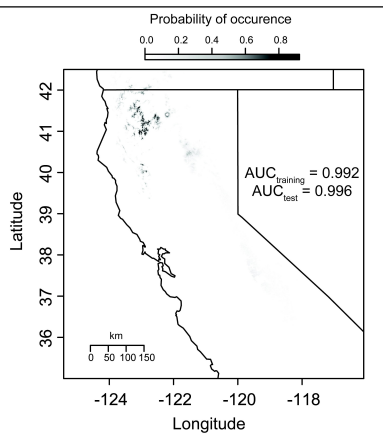
Variable contribution to *P. balfouriana* subsp. *balfouriana* SDM



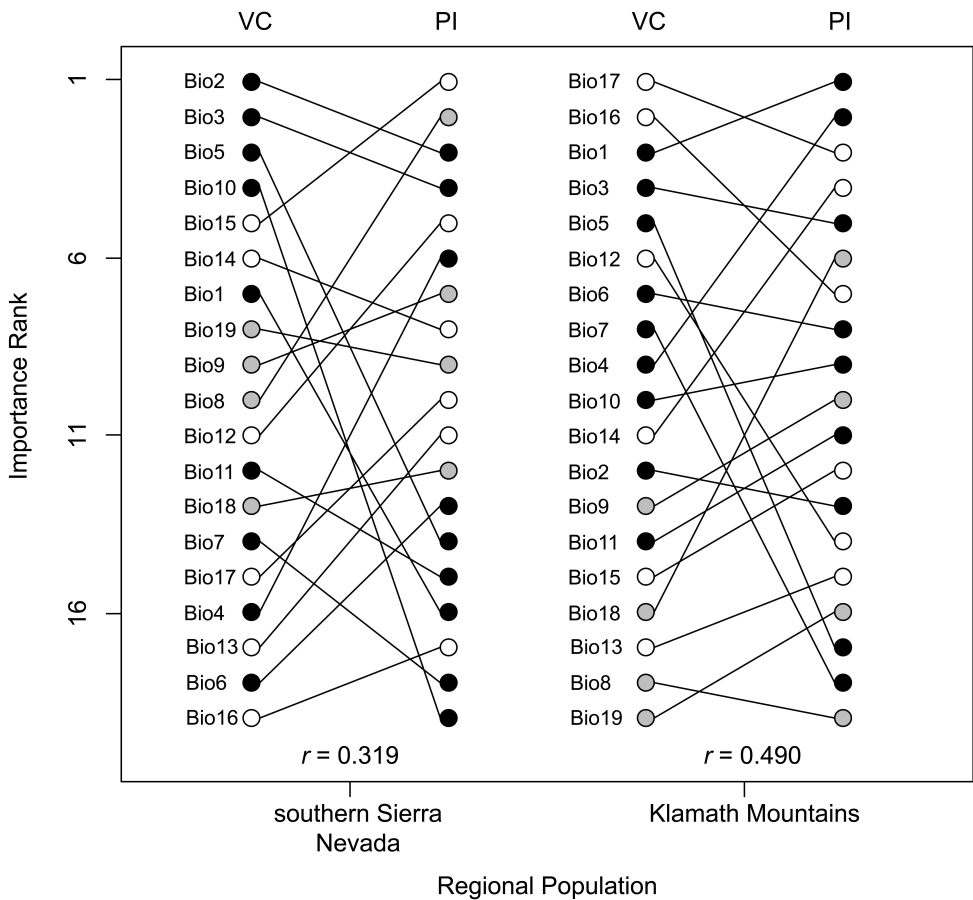
southern Sierra Nevada SDM



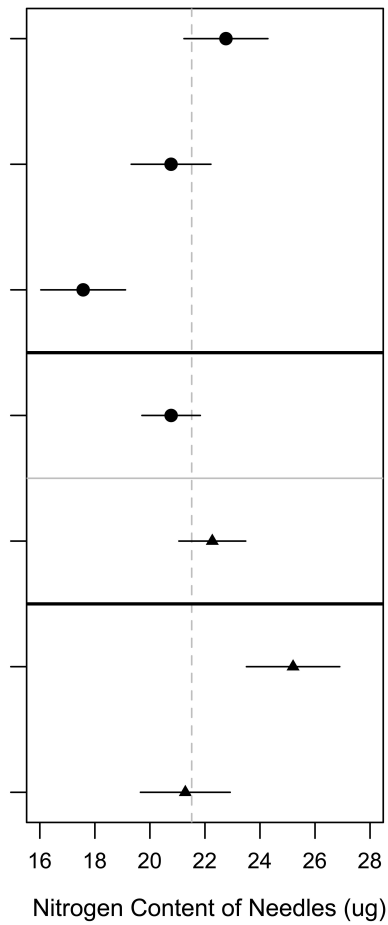
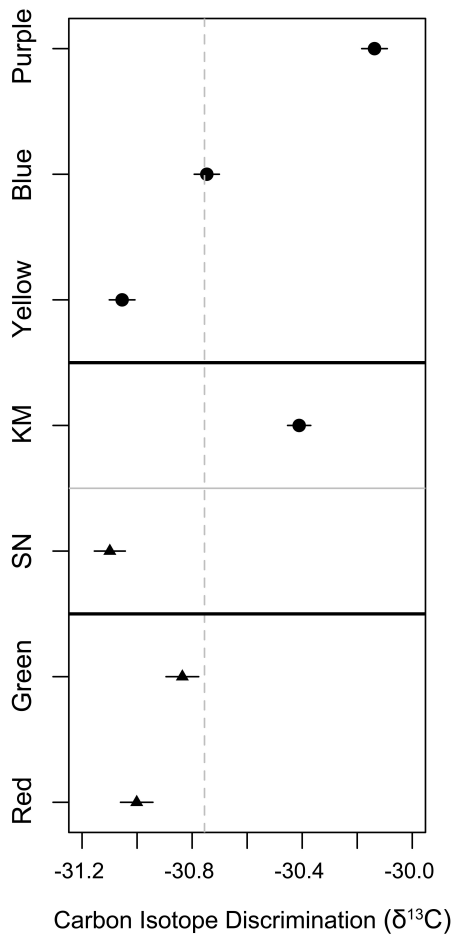
Klamath Mountains SDM

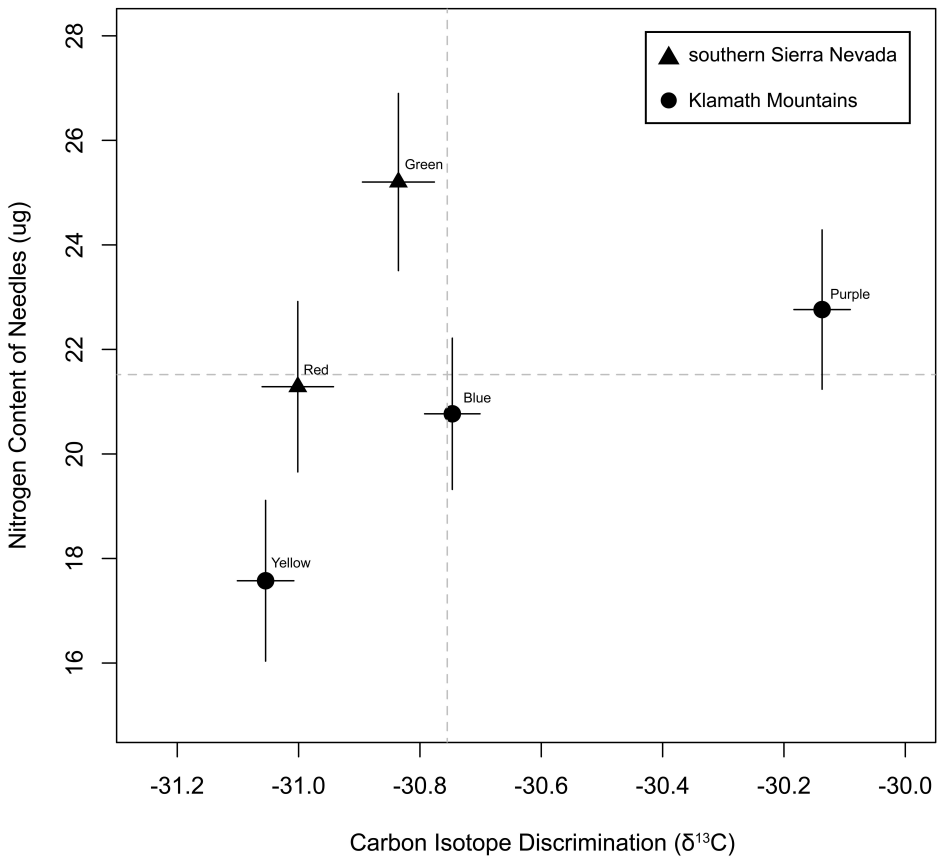


Variable contribution to *P. balfouriana* subsp. *austrina* SDM

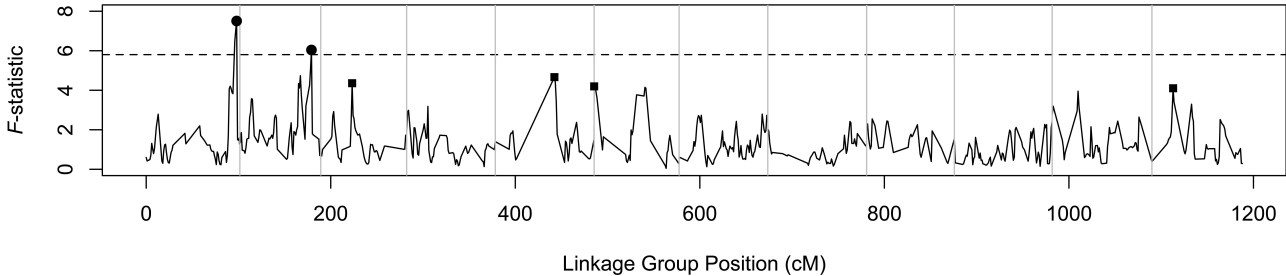


Family or Region





Carbon Isotope Discrimination ($\delta^{13}\text{C}$)



Nitrogen Content of Needles (μg)

